future transportation

MDPI

Article

Towards Green and Smart Ro–Ro Port Terminal Operations: A Comparative Analysis of ICE, BET and e-AGT Tractors

Caterina Malandri, Luca Mantecchini * and Filippo Paganelli

Department of Civil, Chemical, Environmental and Materials Engineering (DICAM), University of Bologna, Viale del Risorgimento 2, 40136 Bologna, Italy; caterina.malandri2@unibo.it (C.M.); filippo.paganelli2@unibo.it (F.P.)
* Correspondence: luca.mantecchini@unibo.it

Abstract

The decarbonization and automation of port operations are emerging as key strategies to enhance the sustainability and efficiency of maritime logistics. This study proposes a simulation-based framework to assess the operational and environmental impacts of transitioning from traditional Internal Combustion Engine (ICE) tractors to Battery Electric Tractors (BET) and Automated Electric Guided Tractors (e-AGT) in Roll-on/Roll-off (Ro–Ro) port terminal operations. The proposed framework is applied to simulate a full vessel turnaround at the Ro–Ro terminal of the Port of Ravenna (Italy). A set of Key Performance Indicators (KPIs) is defined to evaluate turnaround time, vehicle productivity, energy consumption and CO_2 emissions across three scenarios. The results indicate that both BET and e-AGT configurations significantly reduce emissions compared to ICE, with reductions up to 40%. However, the e-AGT scenario reveals operational drawbacks, including increased unloading time and reduced fleet availability due to charging constraints and routing limitations. These findings highlight the environmental potential of automation and electrification but also emphasize the need for integrated planning of fleet size, charging infrastructure and circulation specifications. The proposed framework provides a replicable decision-support tool for port authorities and logistics operators to evaluate alternative handling technologies under realistic conditions.

Keywords: port automation; electric vehicles; Ro–Ro terminal; discrete-event simulation; terminal tractors; CO_2 emissions

Academic Editor: Kum Fai Yuen

Received: 15 July 2025
Revised: 16 August 2025
Accepted: 5 September 2025
Published: 8 September 2025

Citation: Malandri, C.; Mantecchini, L.; Paganelli, F. Towards Green and Smart Ro–Ro Port Terminal Operations: A Comparative Analysis of ICE, BET and e-AGT Tractors. *Future Transp.* **2025**, *5*, 121. https://doi.org/10.3390/futuretransp5030121

1. Introduction

Maritime transport plays a pivotal role in the global freight system, acting as the backbone of international trade by ensuring the movement of vast quantities of goods across long distances at relatively low cost and environmental impact per tonne-kilometre. Within this context, port terminals represent critical nodes where the maritime and land-based components of the supply chain converge, creating a complex intermodal interface. The performance of these nodes directly influences the efficiency, reliability and sustainability of the entire transport network.

Recent studies have shown how congestion, delays and inefficiencies at relevant transport nodes can have cascading effects across supply chains, resulting in increased costs, reduced service quality and elevated environmental externalities [1–3]. In particular, at port terminals vessel turnaround time (i.e., the time a ship spends docked in port for loading and unloading operations) has emerged as a key performance indicator for terminal efficiency. Prolonged turnaround times not only limit port throughput, but also

affect shipping schedules, reduce fleet productivity, and contribute to increased greenhouse gas (GHG) emissions from both ships and handling equipment.

Among the different cargo handling typologies, Roll-on/Roll-off (Ro–Ro) terminals remain relatively understudied, despite their growing strategic relevance. Ro–Ro operations are typically used in the automotive logistics sector or as a flexible alternative to containerized freight, offering faster cargo handling, simplified infrastructure requirements and enhanced modal integration [4]. Thanks to their lower draught and smaller vessel size, Ro–Ro services can serve medium-sized ports, providing additional resilience to the maritime network. However, this operational simplicity comes with unique challenges: Ro–Ro terminal efficiency depends heavily on internal logistics, tractor fleet management, and safe coordination between cargo handling staff and vehicles, often under tight time constraints.

From an environmental standpoint, port authorities and logistics operators are under growing pressure to reduce emissions and embrace low-carbon technologies. The European Green Deal and the FuelEU Maritime Initiative [5] are pushing for decarbonization of maritime transport, including emission reductions in port operations. In this scenario, electrification and automation of handling equipment–already partially adopted in container terminals–are emerging as promising strategies to reduce energy consumption and local pollutants. Nevertheless, most applications of Battery Electric Tractors (BET) and Automated Guided Vehicles (AGVs) have been limited to container settings, while the feasibility and impact of such technologies in Ro–Ro environments remain largely unexplored. Moreover, the current geopolitical and economic context–marked by the lingering effects of the COVID-19 pandemic, the Russia-Ukraine conflict, and energy price volatility–has further emphasized the importance of resilient, efficient and sustainable port operations. In this framework, Ro–Ro terminals may offer greater flexibility and shorter hinterland connectivity times, provided their internal operations are optimized and aligned with technological innovation.

This work advances the state of research by extending simulation-based evaluation to Ro–Ro terminal tractors, integrating operational process modelling with energy-based environmental assessment, a combination not fully addressed in existing studies.

This study is motivated by the lack of comprehensive modelling approaches that simulate Ro–Ro terminal operations during vessel turnaround, especially regarding the comparative performance of traditional Internal Combustion Engine (ICE) tractors, BETs and Automated Guided Electric Tractors (e-AGTs). Existing research has rarely addressed the transport operations carried out by tractors within Ro–Ro terminals, nor has it evaluated the operational trade-offs and environmental implications of introducing electric and automated vehicle fleets in this context. By proposing a simulation framework based on the Element-by-Element (EbE) approach [6] with a real-world application at the Ravenna Ro–Ro terminal (Italy), this study aims to fill a relevant research gap, seeking to offer policy-relevant insights on the interaction between automation, electrification and port-terminal layout design.

The remaining of the paper is organized in the following way. Section 2 contains a literature review on the involved topics, Section 3 describes the model of Ro–Ro terminal operation, Section 4 introduces the application of the proposed approach to a case study. Finally, Section 5 summarizes the main results and findings; conclusions, study limitations and scope for further research on the topic are detailed in Section 6.

2. Literature Review

The simulation of port terminal operations has long represented a critical research area in maritime logistics and transport engineering, owing to the complexity and variability inherent in terminal environments. Broadly, simulation approaches can be classified

into three main categories based on the level of abstraction and analytical granularity: microscopic (discrete-event), mesoscopic, and macroscopic (continuous-flow) models.

Microscopic simulation models, including discrete-event simulation, are widely used in terminal studies due to their capacity to represent detailed interactions between individual agents–such as vehicles, containers, and workers–and infrastructure components (e.g., gates, berths, storage yards). These models allow for high-fidelity tracking of operational sequences, delays, queuing dynamics, and resource constraints, and are particularly suited for assessing Key Performance Indicators such as turnaround time, equipment utilization, and bottlenecks [7–9]. Macroscopic models, in contrast, adopt a system-level perspective by treating flows of goods and/or vehicles in an aggregated manner using continuous variables and differential equations. These models are typically used for strategic planning, demand forecasting or long-term infrastructure assessment and, while less detailed, they offer computational efficiency and the ability to incorporate systemic feedback loops, such as berth congestion effects on maritime routing [10,11]. Mesoscopic models occupy a middle ground by simplifying individual behaviours into probabilistic rules, while preserving relevant aspects of operational sequencing. In recent years, agent-based modelling has also gained relevance in terminal studies, allowing for the representation of autonomous decision-making by individual agents (e.g., vehicles or operators) within complex adaptive systems [12,13]. This approach is especially relevant when evaluating innovative technologies such as autonomous tractors or cooperative scheduling algorithms, where emergent behaviour is difficult to capture using classical discrete-event simulation models. Building on these modelling categories, recent research has explored a range of strategies and operational solutions aimed at improving terminal performance under diverse operational conditions.

Over the past two decades, various strategies have been proposed to enhance port terminal efficiency, ranging from IT-driven optimization of vessel turnaround time and berth allocation, improvements in storage yard management and activity aggregation across different temporal and spatial scales [14–16]. Despite these advancements, integrated models capable of simulating entire terminal systems holistically, especially under conditions of uncertainty, remain challenging to implement effectively [17]. Beyond operational efficiency, increasing attention has been devoted to the environmental dimension of port activities, driven by both regulatory requirements and societal pressure to decarbonise maritime logistics.

The first guideline explicitly dealing with this topic was the EU's 2011 White Paper on transport, which emphasized the urgent need to reduce greenhouse gas (GHG) emissions in freight logistics. More recently, FuelEU Maritime Regulation (EU 2023/1805) mandates a stepwise reduction in the greenhouse gas intensity of powertrain energy sources used by ships calling at EU ports starting from a 2% reduction in 2025 to reach an 80% reduction by 2050. Maritime transport, although relatively efficient in terms of emission per tonne-kilometre, still accounts for approximately 2.3% of global CO_2 emissions, mostly originating from large container and tanker vessels [18,19]. To mitigate this impact, a combination of network-level strategies [20,21] and port-specific initiatives–often involving partnerships between port authorities and shippers–has been adopted, albeit with uneven results [22,23]. Technological interventions span from vessel-based solutions (e.g., cold ironing, automatic mooring) to terminal-level equipment upgrades [24,25]. However, much of this literature remains focused on container terminals, leaving Ro–Ro operations comparatively less explored. Notable exceptions include Jia et al. (2022) [26], who demonstrated the benefits of dual-cycling on turnaround time and CO_2 emissions and a series of studies evaluating the environmental performance of electric and hydrogen-powered terminal tractors in isolated contexts [27–29]. While these technological and policy-driven initiatives have

been extensively investigated in container terminal contexts, their application to Ro–Ro operations, particularly in conjunction with automation, remains comparatively limited.

The integration of automation into Ro–Ro terminal contexts remains particularly limited in the literature. While some studies have considered automation at the level of system architecture or vessel stowage planning [30,31], explicit modelling of automated vehicle performance during terminal operations is lacking. Park et al. (2022) [32] suggest that recent technological advancements, such as AI-driven navigation, could enable autonomous tractors to operate safely in terminal environments, but real-world applications are still at an experimental stage. From a systemic perspective, Ro–Ro services are increasingly recognized as a sustainable intermodal solution, facilitating efficient integration between maritime and road transport [33–35]. Research in this area has primarily focused on system modelling [36], port choice behaviour [37,38], network connectivity [39] and freight flow estimation [40,41]. However, simulation studies tailored to the operational dynamics of Ro–Ro terminals remain sparse. Investigations into terminal capacity [42], origin-destination route capacity [43] and the impact of planning decisions on efficiency and emissions [36] have laid useful groundwork but stop short of modelling tractor-based transport during vessel turnaround.

To summarize, only a limited number of simulation frameworks offer an integrated evaluation of operational and environmental performance in Ro–Ro terminals. When environmental aspects are considered, they typically rely on static emission factors and overlook energy dynamics at the vehicle level. This study addresses that gap by combining a discrete-event simulation of tractor-based operations with a physics-based energy consumption model, enabling a detailed and realistic comparison of alternative handling technologies. Unlike previous port simulation frameworks, our approach links activity-level operational modelling with load-specific energy calculations, providing a high-resolution assessment of both efficiency and emissions in a Ro–Ro terminal context.

3. Methodological Approach

To evaluate the performance of different terminal tractor technologies in a realistic Ro–Ro operational context, this study adopts a simulation-based methodology designed to integrate both operational and environmental dimensions. The proposed approach builds upon the Element-by-Element (EbE) modelling logic and is implemented through a discrete-event simulation environment capable of capturing resource constraints, vehicle interactions and process variability.

The methodology is articulated into a sequence of interdependent phases that reflect the key components of vessel turnaround operations, from berth allocation to yard movements and battery management. Specifically, the following subsections describe: (i) the general structure of the simulation model and its main parameters (Section 3.1), (ii) the modelling of berth and yard activities with a focus on vehicle movements and energy consumption (Section 3.2), and (iii) the definition of Key Performance Indicators (KPIs) used to quantify both operational efficiency and environmental impact (Section 3.3).

3.1. General Modelling Framework

The methodological framework developed in this study aims to evaluate, in an integrated perspective, the operational and environmental performance of internal transport activities in Ro–Ro port terminals during vessel turnaround. As schematically illustrated in Figure 1, the approach is structured into a sequence of interrelated modelling and simulation phases, each contributing to a comprehensive assessment of alternative operational scheme.

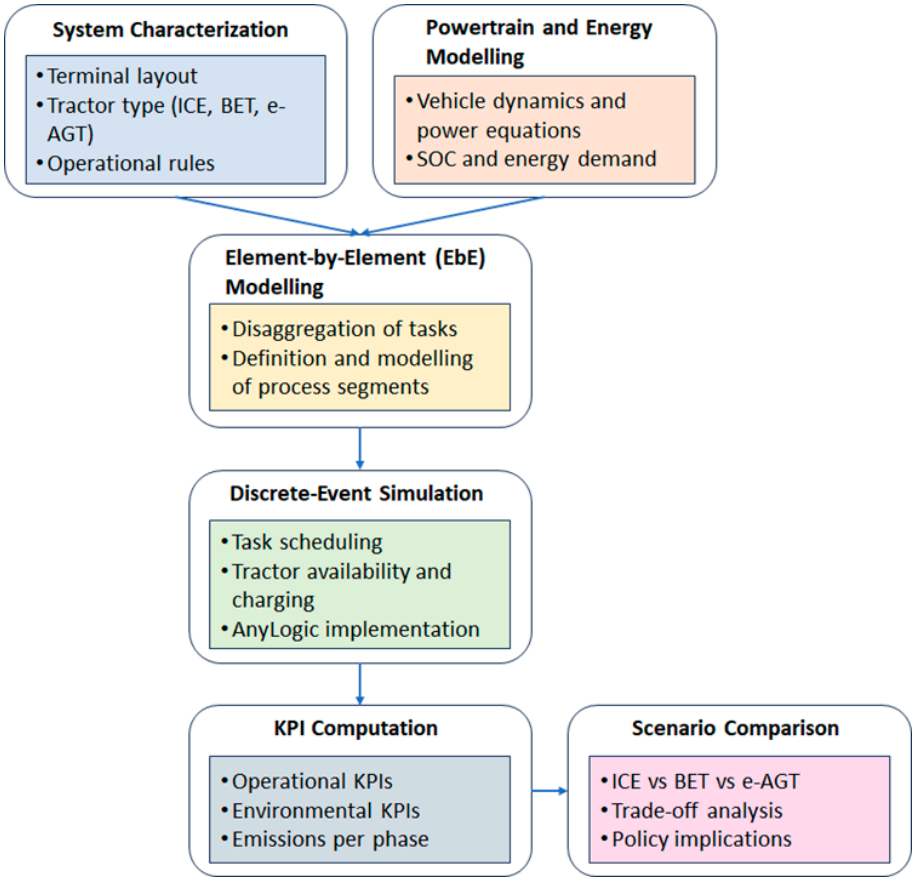

Figure 1. Schematic representation of the methodological framework for the evaluation of operational and environmental performance of transport activities in Ro–Ro terminals.

The first phase involves the definition of the terminal environment and the configuration of the operational processes. This includes the physical layout of the Ro–Ro terminal, the circulation rules for tractors, the characteristics of intermodal transport units (ITUs) and the technical specifications of the three tractor types under comparison–ICE tractors, BETs and e-AGTs. The vessel turnaround cycle is broken down into key operational phases (arrival, unloading, yard movement, loading, departure), which establish the operational boundaries of the model.

The methodological approach enables the disaggregation of terminal processes into elementary activities. Each operation–tractor movement, coupling/de-coupling (hooking/unhooking in the remaining of the paper) of ITUs, loading/unloading, waiting and battery charging–is treated as a distinct process with its own parameters (e.g., duration, energy consumption, distance travelled). This modular structure allows for a detailed and transparent analysis of the contribution of each phase to the terminal's overall performance.

Three scenarios are modelled, each corresponding to a different powertrain configuration: Scenario 1: ICE tractors (baseline); Scenario 2: BETs; Scenario 3: e-AGT tractors with autonomous navigation and modified circulation rules. As described in the following section, the power consumption of each vehicle is modelled using physics-based formulations, accounting for vehicle mass, rolling and aerodynamic resistance and drivetrain efficiency. For electric vehicles, the battery State of Charge (SoC) is dynamically updated based on instantaneous energy use and charging events, incorporating auxiliary power demand and minimum SoC thresholds that trigger recharging.

The dynamic interactions between resources (tractors, charging stations), ITUs and infrastructure are simulated using a discrete-event modelling approach. The simulation accounts for sequential or parallel task execution, resource allocation and queuing, time-

dependent stochasticity of process durations and terminal-specific circulation rules (e.g., one-way loops for e-AGTs). The simulation tracks each tractor's activity in real time, including idle periods, charging events and availability, thus providing an accurate representation of the system under realistic operational conditions. Operational and environmental KPIs are computed throughout the simulation, finally allowing the comparative analysis of the three scenarios, enabling a quantitative assessment of the trade-offs associated with each vehicle technology.

Figure 2 below details the activities related to the vessel arrival and departure cycle (n° arrival/departure ITU) in which the terminal tractor cycle is split into its elementary transport components along with a brief description of the yard and quay transport activities for Ro–Ro terminal tractors, whose characteristics (engine, operation time required to perform certain tasks . . .) have an impact on the energy requirement, the fleet size and the vessel time in port.

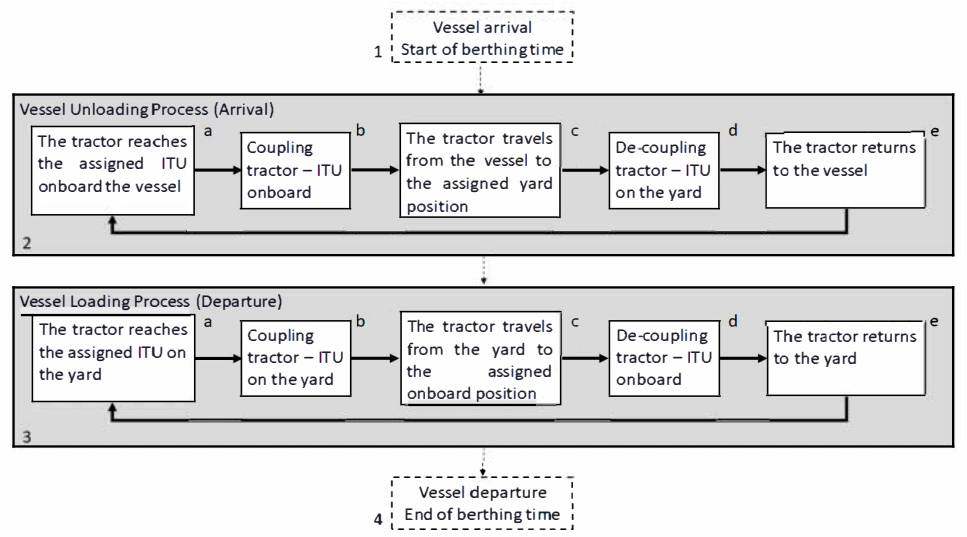

Figure 2. Terminal Tractor cycle for a Ro–Ro vessel turnaround.

If the vessel arrives on schedule (phase 1, Figure 2), pilot and tugboats escort the ship to the assigned berth, which fits the vessel size and draught; otherwise, tug will take place as soon either the service or a suitable berthing point is available. Vessel berth time starts as soon as the ship is berthed. Then, cargo handling staff units unfasten the reef-bands of the unit loads to be unloaded and the vessel unloading process starts (phase 2, Figure 2): freight is disembarked on their wheels (cars and complete vehicles) or by tractors (semitrailers) (2a and 2b, Figure 2) and routed to the storage area (2c, Figure 2) for parking, where the ITU is un-hooked (2d, Figure 2) and left on the yard while the tractors iterate the process (2e, Figure 2) until the arrival process ends.

By the vessel's arrival, export unit loads have already undergone compliance and documentation controls and are in place in the export storage area for the loading phase to begin (phase 3, Figure 2). On yard, terminal tractors reach the assigned ITU (3a, Figure 2) and, after removing standings, hook (3b, Figure 2) and carry them onboard one by one (3c, Figure 2) to the assigned position where the units are un-hooked (3d, Figure 2). Then, the tractors iterate the process (3e, Figure 2) until the loading ends, then the freight is secured to the ships' deck and the vessel waits for clearance. The berthing time ends when the vessel is cleared and the berthing point is left (phase 4, Figure 2). In the following subsections, the details of transport phases performed by tractors during a Ro–Ro vessel turnaround and the relative KPIs are introduced and described.

3.2. Modelling of Berth and Yard Processes

Berth and yard operations in Ro–Ro terminals involve the longitudinal movement of ITUs between the quay and the yard, as well as hooking and unhooking procedures required for vessel loading and unloading. In this study, these processes are modelled through a simulation framework that captures both operational dynamics and energy performance, enabling comparison across different vehicle powertrain technologies.

The simulation replicates the entire vehicle operation cycle, including movement phases during unloading (2a, 2c, 2e in Figure 2) and loading (3a, 3c, 3e), as well as the static phases associated with hooking and unhooking (2b, 2d, 3b, 3d).

The motion phases are characterized using a vehicle energy model, adapted from Fiori et al. (2021) [44], which quantifies the instantaneous power required to overcome inertia, rolling resistance and aerodynamic drag:

$$P_W(t) = \left[(m_{TOT}(t) \cdot a(t)) + (m_{TOT}(t) \cdot g \cdot r_r) + \left(\frac{1}{2} \cdot \rho \cdot C_D \cdot S_f \cdot v(t)^2 \right) \right] \cdot v(t) \quad (1)$$

where $m_{TOT}(t)$ is the total vehicle mass, $a(t)$ and $v(t)$ are acceleration and speed-time functions, g is the gravitation acceleration, r_r is the specific rolling resistance coefficient; ρ is the air density on sea level; S_f and C_D are the frontal cross section area and the body shape coefficient of the vehicle, respectively. Then, $m_{TOT}(t) \cdot a(t)$ is the tractive effort necessary to keep the vehicle in motion; $m_{TOT}(t) \cdot g \cdot r_r$ is the rolling resistance and $\frac{1}{2} \cdot \rho \cdot C_D \cdot S_f \cdot v(t)^2$ is the aerodynamic drag.

The engine power function $P_T(t)$ is expressed by:

$$P_T(t) = \frac{P_W(t)}{\eta_{SH} \cdot \eta_E \cdot \eta_{BAT}} \quad (2)$$

where η_{SH}, η_E and η_{BAT} are the efficiency of the shaft, engine and battery (if present), respectively. In addition, in the case of BET and e-AGT, auxiliary power P_{aux} is also considered. The SoC is dynamically updated during each activity phase:

$$SoC(t) = SoC(0) - \frac{\int_0^t [P_T(t) + P_{aux}] \cdot dt}{Cap_{Bat}} \quad (3)$$

where $\int_0^t [P_T(t) + P_{aux}] \cdot dt$ is the energy used over the time step and Cap_{Bat} is the battery capacity. A threshold value is defined to trigger vehicle recharging. When SoC falls below this threshold, the vehicle enters a charging cycle, during which it becomes unavailable for operation until full charge is restored.

In addition, the specific energy consumption function $EC(t)$ normalized over the time can be expressed by:

$$EC(t) = \frac{\int_0^t [P_T(t) + P_{aux}] \cdot dt}{\int_0^t v(t) \cdot dt} \quad (4)$$

In specific cases, the speed profile $v(t)$ in Equations (1) and (4) can be replaced by average speed or simplified distribution functions; relevant examples can be uncongested contexts such as port quays, storage areas or airport airside [32,45].

The range of battery electric vehicle depends on battery size/capacity, path, driving style, temperature, load and average speed. Recharge can happen at the depot at night (lower power and longer time are required) or in line during idle times (known as "opportunity charge", which involves high power and takes between 5′ and 10′ to be completed). The charging process (path towards the charging station, waiting in the queue and opportunity charge duration) for BET and e-AGT tractors takes place in a charge infrastructure node.

For each performed action (Figure 2), the battery consumption is computed by applying Equation (4) and the residual SoC for each vehicle is updated by means of Equation (3). The rule behind the simulation of the electric battery charge is the comparison between the *j*-th vehicle's residual SoC and a minimum charge threshold (SoC_{min}); if residual SoC > SoC_{min} another operation can be carried out; otherwise, the *j*-th vehicle goes to the charging station, where the SoC is brought back to 100%. The time needed to charge is labelled as CT_j:

$$CT_j = 3600 \frac{(1 - \%SOC_j) \cdot Cap_{Bat}}{P_{charge}} \quad (5)$$

and depends on the residual SoC of the *j*-th vehicle, on the capacity of the battery Cap_{Bat} and on the power output of the charge infrastructure P_{charge}.

3.3. Definition of KPIs for Handling Operation

The evaluation of terminal tractor performance during vessel turnaround requires a structured set of Key Performance Indicators capable of capturing both operational effectiveness and environmental impact. These indicators are defined in alignment with the Element-by-Element modelling approach and serve as the foundation for scenario comparison among different vehicle types.

3.3.1. Operational Time Indicators

Handling activities are disaggregated according to their location (yard or vessel), phase (loading or unloading) and nature (motion or static). Each time component is expressed using the notation T_{uyz}, where $u = \{1 = vessel; 2 = yard\}$; $y = \{1 = loading; 2 = unloading\}$; $z = \{1 = motion; 2 = hooking/unhooking\}$.

From these elementary components, the following cumulative time indicators are derived (Table 1), allowing precise estimation of the tractor fleet's time allocation across operational segments.

Table 1. List of operational time KPIs.

KPI	Description	Structure
T_{OY}	Time On Yard (in motion)	$T_{211} + T_{221}$
T_{OB}	Time On Board (in motion, during loading and unloading)	$T_{111} + T_{121}$
$T_{hook,load}$	Total duration of hooking loading activities—both on-yard and on-board—for which the tractors' speed is zero	$T_{112} + T_{212}$
$T_{hook,unload}$	Total duration of hooking unloading activities—both on-yard and on-board—for which the tractors' speed is zero	$T_{122} + T_{222}$
$T_{hook,vessel}$	Total duration of hooking activities on vessel	$T_{112} + T_{122}$
$T_{hook,yard}$	Total duration of hooking activities on yard	$T_{212} + T_{122}$
T_{hook}	Total duration of hooking activities	$T_{hook,load} + T_{hook,unload}$
Total time on-board	Total working time spent on-board	$T_{OB} + T_{hook,vessel}$
Total time on-yard	Total working time spent on-yard	$T_{OY} + T_{hook,yard}$

3.3.2. Distance-Based Indicators

Each vehicle's path is tracked to compute distance-related KPIs (Table 2), critical for evaluating fleet productivity and estimating energy consumption and emissions.

Table 2. List of operational distance-based KPIs.

KPI	Description
$Km_{on-board}$	Distance travelled on-board, in hooked configuration (lower speed)
$Km_{on-yard}$	Distance in the yard, unhooked (higher speed)
Km_{load}, Km_{unload}	Distance travelled per transport phase
Km_{total}	Total distance travelled by all tractors during vessel turnaround
$Km_{trav,charge}$	Total distance covered to reach the charging station (BET and e-AGT only)

3.3.3. Battery and Charging Performance Indicators (for BET and e-AGT)

For electric vehicles, additional KPIs quantify the impact of battery-charging processes on overall performance (Table 3), reflecting the availability and utilization rate of electric vehicles, as prolonged charging or queuing may lead to temporary service interruptions and reduced fleet efficiency.

Table 3. List of battery and charging KPIs.

KPI	Description
T_{charge}	Total charging time, summing all individual charging events
$T_{trav,charge}$	Total driving time to charging station
$T_{wait,charge}$	Total time spent at charging stations (dependent on infrastructure capacity and fleet demand)

3.3.4. Environmental Indicators

The CO_2 emissions generated during transport and handling are computed through a combined model based on:

- distance travelled at different speeds with corresponding emission factors e_k [gCO_2/km] at the given k-speed (yard and onboard operation take place at different speed);
- hooking/unhooking durations with time-based emission factors e_h [gCO_2/h] during the ITU's hook/unhook phase.
- Total emissions for the entire fleet $E_{CO_2}^{total}$ can be expressed as:

$$E_{CO_2}^{total} = \sum_j (\sum_k e_k \cdot Km_{total,jk} + e_h \cdot T_{hook,j}) \quad (6)$$

where $Km_{total,jk}$ is the distance driven at the given k-speed by the j-th vehicle and $T_{hook,j}$ is the duration of the ITU's hook/unhook phase for the j-th vehicle.

For ICE tractors, the emission factors used in the simulation (gCO_2/km for motion phases and gCO_2/h for static phases) are derived from literature [46,47] and are based on unit emission coefficients expressed in gCO_2 per litre of diesel fuel. For electric vehicles, emissions are computed from energy consumption (kWh) multiplied by the electricity grid emission factor (gCO_2/kWh), also in line with the literature. This approach is consistent with the distance- and time-based structure of the discrete-event simulation and with the available operational data. Nonetheless, the framework can readily incorporate emission factors expressed directly in g/kWh for ICE tractors when detailed engine load profiles are available. Such g/kWh factors, commonly used in thermal machinery emission inventories, relate emissions to the useful mechanical work produced, improve comparability between engines with different efficiencies, and reduce dependence on fuel properties. While the

current activity-based approach aligns with available operational data, it does not explicitly resolve load-specific variations in fuel conversion efficiency as would be possible using a full engine fuel-efficiency map. Incorporating such load-based modelling would represent a valuable extension to refine emission estimates, particularly for scenarios involving different rated powers or duty cycles.

4. Case Study

To validate the proposed methodological framework and assess its applicability to real-world conditions, a case study was implemented at the Ro–Ro terminal of the Port of Ravenna, located in the Emilia-Romagna region, on the Adriatic coast of Italy. This terminal plays a key role within the national and European logistics system, serving as a core node along three of the nine TEN-T corridors. Its strategic positioning ensures multimodal connectivity with northern and central Europe, supported by integrated road and rail infrastructure. The Ro–Ro terminal covers an area of approximately 128,000 square metres, with a storage capacity for about 500 semitrailers and a 473-metre-long quay that allows the handling of a single vessel.

The analysis focuses on the internal operations of the terminal during a complete vessel turnaround cycle involving only semitrailers, which corresponds to the current operational setting of the terminal. The simulation is structured around three distinct scenarios, each representing a different tractor fleet configuration:

- Internal Combustion Engine (ICE) tractors (Scenario 1),
- Battery Electric Tractors (BET) (Scenario 2),
- Automated Electric Guided Tractors (e-AGT) (Scenario 3).

In all scenarios, the number of tractors is kept constant (seven units) and unloading and loading operations are executed sequentially. The circulation within the terminal is bidirectional for ICE and BET vehicles, while a closed-loop, one-way configuration is applied for e-AGT to meet safety and automation requirements.

The simulation incorporates 253 semitrailers to be unloaded and 184 to be loaded, with payloads generated using a triangular distribution (min 15,000 kg, mode 25,000 kg, max 35,000 kg), based on reference literature [48,49]. The semitrailer arrival process follows a negative exponential distribution to replicate real-world traffic peaks and weight/documentation controls are assumed at the entry point. Onboard cargo handling activities are estimated to last 1 h and 18 min, in line with practices directly observed at the terminal. All simulation experiments are repeated across 20 iterations to ensure statistical robustness and allow for scenario comparison. The location of the Port of Ravenna and the layout of its Ro–Ro terminal used to implement the simulation are represented in Figures 3 and 4, respectively.

Each tractor type is characterized by specific technical parameters related to engine power, weight, speed profiles, emissions and–where applicable–battery performance. ICE tractors operate with 320 kW engines and emission factors of 1053 gCO_2/km onboard and 800 gCO_2/km in yard segments. It should be noted that the 320 kW value refers to the maximum rated engine power of a high-spec yard tractor model. In typical Ro–Ro operations, actual power demand is significantly lower and well within the capabilities of smaller ICE tractors in the 200–220 kW range, which are commercially available and could perform the analyzed tasks with minor trade-offs in acceleration margins and hill-climb performance. BET and e-AGT tractors are modelled with 110 kW engines, and their environmental impact is computed indirectly through energy consumption and the assumed electricity emission factor. Specific emission factor in motion [gCO_2/km] for ICE, BET and e-AGT have been derived by the literature for both yard (speed V1) and onboard (speed V2) configurations [48,49]. Specific emission factor in standstill position

(i.e., speed V4 = 0) [gCO_2/h] for semitrailer hook/unhook phases and the duration of hooking activities are also derived by the literature [32,36]. The average speeds used in the simulation are set according to operational constraints–such as yard traffic conditions, routing inside the vessel, safety regulations, and maneuvering phases–and are not limited by the rated engine power.

Figure 3. Location map of Ravenna port and Ro–Ro terminal.

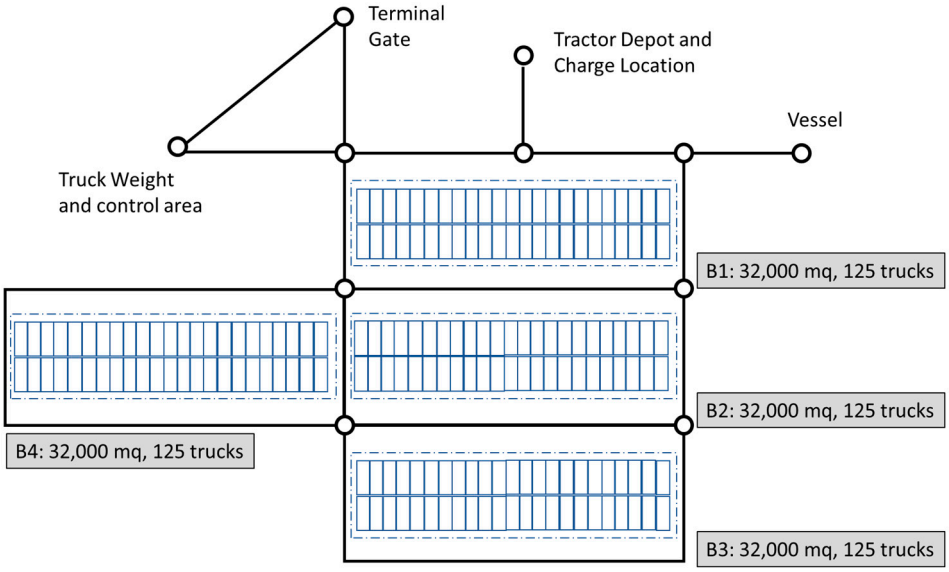

Figure 4. Layout of the Ro–Ro terminal used for the simulation.

The e-AGT scenario additionally integrates a reduced and constant operating speed and an optimized circulation scheme designed to minimize conflicts and vehicle interactions, leveraging onboard sensing systems. Battery-powered vehicles (BET and e-AGT) are subject to dynamic State of Charge tracking during the simulation. Recharging is triggered when the SoC drops below a minimum threshold of 15% and the corresponding recharge process includes vehicle repositioning, queuing (when infrastructure is occupied) and charging time, which follows a triangular distribution (20–30 min, mode: 25 min). The simulation assumes that only two vehicles can charge simultaneously, thus introducing potential delays in fleet availability depending on charging demand and vehicle rotation. The auxiliary power demand of electric vehicles and the impact of charging cycles on operation times are explicitly represented. Hook and unhook semitrailer time follow a normal distribution, while semitrailer payload follows a triangular distribution. See Table 4 for a summary of the mentioned characteristics.

Table 4. Tractor and semitrailer characteristics.

	ICE-Scenario 1	BET-Scenario 2	e-AGT-Scenario 3
Weight [kg]	12,000	12,000	12,000
Power [kW]	320	110	110
Speed [km/h]	V1 = N (16; 3) V2 = N (10; 3)	V1 = N (16; 3) V2 = N (10; 3)	V3 = K (10; 0)
e_k [gCO_2/km]	1053.33 (V1) 800 (V2)	700 (V1) 560 (V2)	560 (V3)
e_h [gCO_2/h]	600 (V4)	420 (V4)	420 (V4)
Battery charge time	n/a	t = TR (20; 30; 25) min	t = TR (20; 30; 25) min
SoC_{min}	n/a	15%	15%
Semitrailer payload [kg]	w = TR (15,000; 35,000; 25,000)		
Semitrailer hook time [min]	t_h = N (1.55; 0.724)		
Semitrailer unhook time [min]	t_{uh} = N (1.09; 0.515)		

The model is implemented in AnyLogic, a discrete-event and agent-based simulation environment suitable for representing complex, resource-constrained systems such as port terminals. The simulation accounts for all stages of the turnaround cycle, including stevedoring, internal yard transport, ITU hooking/unhooking, vehicle queuing and routing and battery management. Randomness is introduced in payload distributions, driving times, energy consumption and recharging events to reflect realistic variability. Initial conditions assume vessel arrival at 09:00, with unloading beginning at 10:18. All tractors are available at the start of the operation. For BET and e-AGT, SoC levels are initialized at 100%.

The validation of the proposed framework is carried out on two complementary levels. From a methodological perspective, the modelling architecture, combining discrete-event simulation of Ro–Ro terminal operations with a physics-based energy consumption module, is grounded in established approaches from the literature and implemented using parameters and formulations consistent with recognized engineering practices. This ensures internal validity and theoretical robustness. From an application perspective, the case study is tested against observed operational data from the Port of Ravenna. In particular, key performance indicators from the baseline ICE scenario, including vessel turnaround time, average tractor travel distances, hooking/unhooking durations and fleet utilization rates, are compared to terminal records and direct observations. Furthermore, all physical and environmental parameters, such as tractor speeds, payload distributions, battery characteristics and emission factors, are cross-checked against peer-reviewed sources and manufacturer specifications to ensure plausibility.

The simulation is designed to capture the interaction between operational parameters (e.g., circulation logic, fleet utilization, layout configuration) and environmental indicators (e.g., energy consumption, charging behaviour, CO_2 emissions), allowing for a comprehensive and comparative evaluation of the performance of conventional, electric and automated handling fleets.

5. Results and Discussion

The simulation outcomes provide a detailed comparison of the operational and environmental performance of three considered types of terminal tractors during a complete Ro–Ro vessel turnaround cycle at the Ravenna terminal. Results are analyzed according to key performance indicators (KPIs) grouped into three categories: turnaround time and fleet performance, distance travelled and activity distribution and CO_2 emissions.

In terms of vessel turnaround time, the adoption of BETs and e-AGTs introduces notable variations (Table 5). While BETs yield performance similar to ICE tractors in both unloading and loading phases, e-AGTs show a significant increase in total Ship Unloading Time (SUT), rising from 6:13 h in the ICE scenario to 8:28 h. The difference in Ship Loading Time (SLT) is less pronounced (from 5:38 to 6:08 h). This discrepancy is largely attributable to the lower average speed and the mandatory unidirectional circulation rule applied to e-AGTs for safety reasons. Moreover, the need for battery recharging imposes additional constraints, as tractors temporarily exit service during the charging process. For e-AGTs, the total time spent on battery charging exceeds 5 h and 50 min, with over 3 h lost due to queuing at the charging station. This sharply contrasts with the ICE tractors baseline, which requires no interruptions.

Table 5. Simulation outputs: effects on vessel turnaround time.

	ICE	BET	e-AGT
Ship Unloading Time SUT [hh:mm]	06:13	06:05	08:28
Ship Loading Time SLT [hh:mm]	05:38	05:46	06:08
T_{charge} [hh:mm]	n/a	02:53	05:53
$T_{trav,charge}$ [hh:mm]	n/a	00:09	00:37
$T_{wait,charge}$ [hh:mm]	n/a	01:57	03:08

Fleet productivity, measured by total distance travelled and number of completed trips per vehicle, shows minor variation across scenarios (Table 6). Despite the circulation constraints imposed on e-AGTs, the total distance covered remains comparable across vehicle types, suggesting that the relatively compact size of the terminal layout mitigates the inefficiencies associated with longer routing paths. However, e-AGTs exhibit longer cumulative time on the yard (T_{OY} in Table 6), which rises from 32:26 h (ICE) to over 50:48 h. This increase is due not only to lower speed but also to multiple recharging cycles required within a single operation window. The high uniformity in trip distribution among tractors also leads to synchronized recharging needs, causing temporary halts in operation when no vehicle is available. The hooking and unhooking operations (T_{hook} in Table 6) represent a significant share of total tractor activity time in all scenarios, exceeding 21 h in each case. These activities, although static from a spatial perspective, impose energy or fuel consumption–especially for ICE tractors–due to engine idling and auxiliary system use. The overall pattern reveals a consistent time burden across vehicle types, indicating that automation (e.g., e-AGT) does not currently provide significant time savings in this phase, likely due to conservative operational assumptions adopted to reflect real-world safety standards.

Regarding environmental performance, results highlight substantial reductions in CO_2 emissions when transitioning from ICE to electric alternatives (Table 7). Total emissions fall from approximately 616,000 gCO_2 (ICE) to 420,000 gCO_2 (BET), corresponding to a 31.8% reduction. The e-AGT scenario achieves the highest environmental benefit, with total emissions reduced by 40% compared to ICE. When normalized per ITU, the emissions decrease from 1409 gCO_2/ITU (ICE) to 846 gCO_2/ITU (e-AGT). A further normalization by total payload confirms this trend, with the unit emission falling from 0.038 to 0.023 gCO_2/kg. These values are consistent with existing studies in container terminal contexts [48,49] and confirm the potential of automated electric vehicles to support port decarbonization strategies.

Table 6. Simulation outputs: effects on fleet productivity.

	ICE [hh:mm:ss]	**BET [hh:mm:ss]**	**e-AGT [hh:mm:ss]**
T_{111}	14:16:59	14:05:22	13:51:37
T_{112}	05:08:19	05:25:11	05:07:29
T_{121}	16:02:23	16:02:23	16:42:35
T_{122}	06:55:49	07:02:49	06:54:49
T_{211}	11:14:13	11:23:18	17:28:56
T_{212}	03:40:41	03:02:24	03:08:36
T_{221}	21:12:21	21:16:23	23:22:22
T_{222}	05:38:23	05:38:23	06:48:20
T_{OB}	30:19:22	30:07:45	30:34:12
T_{OY}	32:26:34	32:39:41	40:51:18
T_{hook}	21:22:47	21:08:47	21:58:47
Total time on board	42:23:45	42:35:45	42:36:45
Total time on yard	41:45:38	41:20:28	50:48:14

Table 7. Simulation outputs: environmental effects.

	ICE	**BET**	**e-AGT**
$E_{CO_2}^{total}$ [gCO_2]	615,986	420,345	369,857
$E_{CO_2}^{total/ITU}$ [gCO_2/ITU]	1.409	0.961	0.846
$E_{CO_2}^{total/kg}$ [gCO_2/kg]	0.038	0.026	0.023

However, the environmental gains come at the expense of operational reliability and turnaround time, particularly in the case of e-AGT. The results suggest that without a sufficient number of vehicles or charging stations, the adoption of automation may undermine service levels–especially under high traffic volumes or when multiple vessels are handled in parallel. The simulation shows that even under current single-vessel operations, fleet availability becomes a limiting factor when recharging needs overlap. Unless compensated by fleet expansion, increased charging capacity, or operational adjustments (e.g., lower SoC thresholds, opportunity charging during idle phases), terminal efficiency may deteriorate.

These trade-offs underscore the importance of infrastructure planning and charging station dimensioning when transitioning to electric or automated handling fleets. The closed-loop circulation rule adopted for e-AGT, while justified from a safety perspective, also emerges as a critical factor limiting productivity. In larger terminals or under more complex operational conditions, its impact would likely be even more pronounced. Overall, the case study highlights the feasibility of electrification and automation in Ro–Ro terminal operations from an environmental standpoint but also emphasizes the need for careful integration of supporting infrastructure and adaptive operational strategies. The simulation framework proves effective in quantifying both operational bottlenecks and emission savings, providing port authorities and terminal operators with a decision-support tool to guide technology adoption under realistic conditions

6. Conclusions

This study presented a simulation-based framework to evaluate the operational and environmental performance of Ro–Ro terminal tractors powered by internal combustion engines, battery electric systems and automated electric guided technologies. Using the Element-by-Element modelling approach and a discrete-event simulation environment, the study captured the detailed dynamics of vessel turnaround operations at the Ro–Ro

terminal of the Port of Ravenna, offering a realistic assessment of the trade-offs introduced by electrification and automation.

The results show that the transition from conventional diesel tractors to electric and automated vehicles has the potential to significantly reduce CO_2 emissions, with BET and e-AGT fleets achieving emission reductions of approximately 32% and 40%, respectively, compared to the ICE baseline. When normalized per transported ITU or per unit of payload, these savings confirm the strong environmental benefit of adopting zero-emission yard handling technologies. From an operational standpoint, however, the advantages of automation are less clear-cut. While BET vehicles performed comparably to ICE tractors in terms of turnaround time and fleet productivity, the e-AGT scenario was associated with longer unloading durations, increased yard activity time and higher sensitivity to battery-charging constraints. The combination of reduced speeds, circulation constraints (unidirectional routing) and limited charging infrastructure led to lower vehicle availability and potentially introduced delays, particularly during high-demand phases. Future extensions of the model will incorporate advanced charging management strategies, such as opportunity charging during operational idle periods and dynamic SoC thresholding, to evaluate their potential in reducing queue times and improving the operational performance of automated electric fleets.

These findings underscore the importance of holistic planning when introducing electric and automated technologies in port environments; in fact, infrastructure dimensioning, fleet sizing and process redesign must be considered in parallel to avoid unintended consequences on service levels. While electrification appears readily feasible with limited operational disruption, full automation requires more careful integration, particularly in legacy terminals with spatial or organizational constraints. Nonetheless, several limitations of the present study should be acknowledged. First, the simulation focuses on a single vessel turnaround and a fixed number of handling vehicles, which may not fully capture the variability and complexity of multi-ship or high-traffic scenarios. Second, behavioural aspects such as operator decision-making, dynamic task reassignment and real-time prioritization are not explicitly modelled, potentially underestimating the adaptability of human-operated systems. Third, the environmental impact assessment is limited to operational CO_2 emissions and does not include a full life-cycle perspective, such as emissions from vehicle manufacturing, battery production, or end-of-life disposal. Finally, assumptions regarding charging infrastructure (e.g., station capacity, power output, vehicle scheduling) are simplified and should be refined through collaboration with terminal operators and technology providers.

The framework has been validated both methodologically–through alignment with established modelling approaches and parameterization from peer-reviewed sources–and empirically, via comparison with observed operational data from the Port of Ravenna. While these steps support the reliability of the results under the defined assumptions, further applications to multiple terminals and diverse operating conditions would strengthen the external validity of the approach.

Despite these limitations, the simulation framework developed offers a flexible and transparent tool to support scenario analysis and decision-making in Ro–Ro terminal planning. Future research may extend this work by incorporating stochastic demand patterns, assessing hybrid fleet configurations, or applying the model to terminals with different spatial layouts and regulatory constraints. Additionally, the integration of life-cycle sustainability metrics and energy grid decarbonization scenarios would enable a more comprehensive evaluation of long-term impacts.

Author Contributions: Conceptualization, C.M., L.M. and F.P.; methodology, C.M., L.M. and F.P.; software, C.M.; validation, C.M., L.M.; formal analysis, C.M., L.M. and F.P.; investigation, L.M. and F.P.; resources, C.M., L.M. and F.P.; data curation, C.M. and F.P.; writing—original draft preparation, C.M., L.M. and F.P.; writing—review and editing, C.M. and L.M.; visualization, C.M., L.M. and F.P.; supervision, L.M. All authors have read and agreed to the published version of the manuscript.

Funding: This research received no external funding.

Institutional Review Board Statement: Not applicable.

Informed Consent Statement: Not applicable.

Data Availability Statement: Dataset available on request from the authors.

Conflicts of Interest: The authors declare no conflicts of interest.

Abbreviations

The following abbreviations are used in this manuscript:

Ro–Ro	Roll-on–Roll-off
ICE	Internal Combustion Engine
BET	Battery Electric Tractors
e-AGT	Automated Electric Guided Tractors
AGV	Automated Guided Vehicle
GHG	Greenhouse Gas
KPI	Key Performance Indicator
EbE	Element-by-Element
ITU	Intermodal Transport Unit
SoC	State of Charge
SUT	Ship Unloading Time
SLT	Ship Loading Time

References

1. Damgacioglu, H.; Celik, N.; Guller, A. A route-based network simulation framework for airport ground system disruptions. *Comput. Ind. Eng.* **2018**, *124*, 449–461. [CrossRef]
2. Gu, Y.; Fu, X.; Liu, Z.; Xu, X.; Chen, A. Performance of transportation network under perturbations: Reliability, vulnerability, and resilience. *Transp. Res. Part E Logis. Transp. Rev.* **2020**, *133*, 101809. [CrossRef]
3. Postorino, M.N.; Mantecchini, L.; Malandri, C.; Paganelli, F. A methodological framework to evaluate the impact of disruptions on airport turnaround operations: A case study. *Case Stud. Transp. Pol.* **2020**, *8*, 429–439. [CrossRef]
4. Dias, J.Q.; Calado, J.M.F.; Mendonça, M.C. The role of European «ro-ro» port terminals in the automotive supply chain management. *J. Transp. Geogr.* **2010**, *18*, 116–124. [CrossRef]
5. Decarbonising Maritime Transport—FuelEU Maritime. Available online: https://transport.ec.europa.eu/transport-modes/maritime/decarbonising-maritime-transport-fueleu-maritime_en (accessed on 15 July 2025).
6. Postorino, M.N.; Mantecchini, L. An element-by-element approach for a holistic estimation of the airport carbon footprint. In *Sustainable Aviation. Greening the Flight Path*; Palgrave Macmillan, Springer International Publishing—Springer Nature: Cham, Switzerland, 2020; pp. 193–214.
7. De Luca, S.; Cantarella, G.E.; Cartenì, A. A macroscopic model of a container terminal based on diachronic networks. In *Schedule-Based Modeling of Transportation Networks: Theory and Applications*; Nuzzolo, A., Wilson, N.H.M., Eds.; Springer Science: New York, NY, USA, 2009; pp. 285–310.
8. Yun, W.Y.; Choi, Y.S. A simulation model for container-terminal operation analysis using an object-oriented approach. *Int. J. Prod. Econ.* **1999**, *59*, 221–230. [CrossRef]
9. Henesey, L.; Davidsson, P.; Persson, J.A. Evaluation of automated guided vehicle systems for container terminals using multi agent based simulation. In *International Workshop on Multi-Agent Systems and Agent-Based Simulation*; Springer: Berlin/Heidelberg, Germany, 2008; pp. 85–96.
10. Gambardella, L.M.; Rizzoli, A.E.; Zaffalon, M. Simulation and planning of an intermodal container terminal. *Simulation* **1998**, *71*, 107–116. [CrossRef]

11. Murty, K.G.; Liu, J.; Wan, Y.W.; Linn, R. A decision support system for operations in a container terminal. *Decis. Support Syst.* **2005**, *39*, 309–332. [CrossRef]
12. Muravev, D.; Hu, H.; Rakhmangulov, A.; Mishkurov, P. Multi-agent optimization of the intermodal terminal main parameters by using AnyLogic simulation platform: Case study on the Ningbo-Zhoushan Port. *Int. J. Inf. Manag.* **2021**, *57*, 102133. [CrossRef]
13. Fransen, R.W.; Davydenko, I.Y. Empirical agent-based model simulation for the port nautical services: A case study for the Port of Rotterdam. *Marit. Transp. Res.* **2021**, *2*, 100040. [CrossRef]
14. Preston, P.; Kozan, E. An approach to determine storage locations of containers at seaport terminals. *Comput. Oper. Res.* **2001**, *28*, 983–995. [CrossRef]
15. Cartenì, A.; de Luca, S. Simulation of a container terminal through a discrete event approach: Literature review and guidelines for application. In Proceedings of the European Transport Conference, Noordwijkerhout, The Netherlands, 5–7 October 2009.
16. Abu Aisha, T.; Ouhimmou, M.; Paquet, M.; Montecinos, J. Developing the seaport container terminal layout to enhance efficiency of the intermodal transportation system and port operations–case of the Port of Montreal. *Marit. Policy Manag.* **2022**, *49*, 181–198. [CrossRef]
17. Lu, Y.; Fang, S.; Chen, G.; Niu, T.; Liao, R. Cyber-physical integration for future green seaports: Challenges, state of the art and future prospects. *IEEE Trans. Ind. Cyber-Phys. Syst.* **2023**, *1*, 21–43. [CrossRef]
18. International Transport Forum. 2014. Available online: https://www.itf-oecd.org/2014-annual-summit-highlights-transport-changing-world-session-summaries (accessed on 5 September 2025).
19. Nunes, R.A.O.; Alvim-Ferraz, M.C.M.; Martins, F.G.; Sousa, S.I.V. Assessment of shipping emissions on four ports of Portugal. *Environ. Pollut.* **2017**, *231*, 1370–1379. [CrossRef] [PubMed]
20. Psaraftis, H.N.; Kontovas, C.A. Speed models for energy-efficient maritime transportation: A taxonomy and survey. *Transp. Res. Part C Emerg.* **2013**, *26*, 331–351. [CrossRef]
21. Andersson, P.; Ivehammar, P. Green approaches at sea—The benefits of adjusting speed instead of anchoring. *Transp. Res. Part D Transp. Environ.* **2017**, *51*, 240–249. [CrossRef]
22. Castellano, R.; Ferretti, M.; Musella, G.; Risitano, M. Evaluating the economic and environmental efficiency of ports: Evidence from Italy. *J. Clean. Prod.* **2020**, *271*, 122560. [CrossRef]
23. Alamoush, A.S.; Olcer, A.I.; Ballini, F. Ports' role in shipping decarbonization: A common port incentive scheme for shipping greenhouse gas emission reduction. *Clean. Logist. Supply Chain* **2022**, *3*, 100021. [CrossRef]
24. Yang, Y.C.; Chang, W.M. Impacts of electric rubber-tired gantries on green port performance. *Res. Transp. Bus. Manag.* **2013**, *8*, 67–76. [CrossRef]
25. Vlahopoulos, D.; Bouhouras, A.S. Solution for RTG crane power supply with the use of a hybrid energy storage system based on literature review. *Sustain. Energy Technol. Assess.* **2022**, *52*, 102351. [CrossRef]
26. Jia, B.; Tierney, K.; Reinhardt, L.B.; Pahl, J. Optimal dual cycling operations in roll-on roll-off terminals. *Transp. Res. Part E Logist. Transp. Rev.* **2022**, *159*, 102646. [CrossRef]
27. Di Ilio, G.; Di Giorgio, P.; Tribioli, L.; Bella, G.; Jannelli, E. Preliminary design of a fuel cell/battery hybrid powertrain for a heavy-duty yard truck for port logistics. *Energy Convers. Manag.* **2021**, *243*, 114423. [CrossRef]
28. Sato, S.; Jiang, Y.J.; Russell, R.L.; Miller, J.W.; Karavalakis, G.; Durbin, T.D.; Johnson, K.C. Experimental driving performance evaluation of battery-powered medium and heavy duty all-electric vehicles. *Int. J. Elect. Power* **2022**, *141*, 108100. [CrossRef]
29. Chang, C.C.; Huang, P.C.; Tu, J.S. Life cycle assessment of yard tractors using hydrogen fuel at the Port of Kaohsiung, Taiwan. *Energy* **2019**, *189*, 116222. [CrossRef]
30. Park, S.; Hwang, J.; Yang, H.; Kim, S. Simulation modelling for automated guided vehicle introduction to the loading process of ro-ro ships. *J. Mar. Sci. Eng.* **2021**, *9*, 441. [CrossRef]
31. Sun, X.; Wang, S.; Wang, Z.; Liu, C.; Yin, Y. A semi-automated approach to stowage planning for Ro-Ro ships. *Ocean Eng.* **2022**, *247*, 110648. [CrossRef]
32. Park, S.H.; Hwang, J.; Yun, S.; Kim, S. Automatic Guided Vehicles Introduction Impacts to Roll-On/Roll-Off Terminals: Simulation and Cost Model Analysis. *J. Adv. Transp.* **2022**, *1*, 6062840. [CrossRef]
33. Fiori, C.; Marzano, V. Modelling energy consumption of electric freight vehicles in urban pickup/delivery operations: Analysis and estimation on a real-world dataset. *Transp. Res. Part D Transp. Environ.* **2018**, *65*, 658–673. [CrossRef]
34. Christodoulou, A.; Raza, Z.; Woxenius, J. The integration of RoRo shipping in sustainable intermodal transport chains: The case of a North European RoRo service. *Sustainability* **2019**, *11*, 2422. [CrossRef]
35. Raza, Z.; Woxenius, J.; Finnsgård, C. Slow steaming as part of SECA compliance strategies among RoRo and RoPax shipping companies. *Sustainability* **2019**, *11*, 1435. [CrossRef]
36. Iannone, R.; Miranda, S.; Prisco, L.; Riemma, S.; Sarno, D. Proposal for a flexible discrete event simulation model for assessing the daily operation decisions in a Ro–Ro terminal. *Simul. Model. Pract. Theory* **2016**, *61*, 28–46. [CrossRef]
37. Mangan, J.; Lalwani, C.; Gardner, B. Modelling port/ferry choice in RoRo freight transportation. *Int. J. Transp. Manag.* **2002**, *1*, 15–28. [CrossRef]

38. Görçün, Ö.F.; Küçükönder, H. An integrated MCDM approach for evaluating the Ro-Ro marine port selection process: A case study in black Sea region. *Aust. J. Marit. Ocean. Aff.* **2021**, *13*, 203–223. [CrossRef]
39. de Langen, P.W.; Udenio, M.; Fransoo, J.C.; Helminen, R. Port connectivity indices: An application to European RoRo shipping. *J. Shipp. Trade* **2016**, *1*, 6. [CrossRef]
40. Cascetta, E.; Marzano, V.; Papola, A.; Vitillo, R. A multimodal elastic trade coefficients MRIO model for freight demand in Europe. In *Freight Transport Modelling*; Besn-Akiva, M., Meersman, H., Van de Voorde, E., Eds.; Emerald Group Publishing Limited: Leeds, UK, 2013; pp. 45–68.
41. Antoniou, C.; Barceló, J.; Breen, M.; Bullejos, M.; Casas, J.; Cipriani, E.; Ciuffo, B.; Djukic, T.; Hoogendoorn, S.; Marzano, V.; et al. Towards a generic benchmarking platform for origin destination flows estimation/updating algorithms: Design, demonstration and validation. *Transp. Res. Part C Emerg.* **2016**, *66*, 79–98. [CrossRef]
42. Morales-Fusco, P.; Saurí, S.; Spuch, B. Quality indicators and capacity calculation for RoRo terminals. *Transp. Plann. Technol.* **2010**, *33*, 695–717. [CrossRef]
43. Özkan, E.D.; Nas, S.; Guler, N. Capacity Analysis of Ro-Ro Terminals by Using Simulation Modeling Method. *Asian J. Shipp. Logist.* **2016**, *32*, 139–147. [CrossRef]
44. Fiori, C.; Montanino, M.; Nielsen, S.; Seredynski, M.; Viti, F. Microscopic energy consumption modelling of electric buses: Model development, calibration, and validation. *Transp. Res. D Transp. Environ.* **2021**, *98*, 102978. [CrossRef]
45. Postorino, M.N.; Mantecchini, L.; Gualandi, E. Integration between aircraft and handling vehicles during taxiing procedures to improve airport sustainability. *Int. J. Transp. Dev. Integr.* **2017**, *1*, 28–42. [CrossRef]
46. Nykvist, B.; Olsson, O. The feasibility of heavy battery electric trucks. *Joule* **2021**, *5*, 901–913. [CrossRef]
47. Budiyanto, M.A.; Huzaifi, M.H.; Sirait, S.J.; Prayoga, P.H.N. Evaluation of CO_2 emissions and energy use with different container terminal layouts. *Sci. Rep.* **2021**, *11*, 5476. [CrossRef]
48. Ecker, M.; Shafiei, S.P.; Sauer, D.U. Influence of operational condition on lithium plating for commercial lithium-ion batteries—Electrochemical experiments and post-mortem-analysis. *Appl. Energy* **2017**, *206*, 934–946. [CrossRef]
49. Al-Ogaili, A.S.; Ramasamy, A.; Hashim, T.J.T.; Al-Masri, A.N.; Hoon, Y.; Jebur, M.N.; Verayiah, R.; Marsadek, M. Estimation of the energy consumption of battery driven electric buses by integrating digital elevation and longitudinal dynamic models: Malaysia as a case study. *Appl. Energy* **2020**, *280*, 115873. [CrossRef]